Molecular Crystals and Liquid Crystals
Publication details, including instructions for authors and subscription information:
http://www.tandfonline.com/loi/gmcl16

SRS Radiation Induced Polymerization of 2,4-Hexadiynediol-BIS-(p-Toluenesulphonate) (PTS)

Michael Dudley [a] , John N Sherwood [a] , David J Ando [b] & David Bloor [b]

[a] Department of Pure and Applied Chemistry, University of Strathclyde, 295 Cathedral Street, GLASGOW, G1 1XL, Scotland

[b] Department of Physics, Queen Mary College, University of London, Mile End Road, LONDON, E1 4NS, England

Version of record first published: 17 Oct 2011.

To cite this article: Michael Dudley , John N Sherwood , David J Ando & David Bloor (1983): SRS Radiation Induced Polymerization of 2,4-Hexadiynediol-BIS-(p-Toluenesulphonate) (PTS), Molecular Crystals and Liquid Crystals, 93:1, 223-237

To link to this article: http://dx.doi.org/10.1080/00268948308073530

Mol. Cryst. Liq. Cryst., 1983, Vol. 93, pp. 223–237
0026-8941/83/9304–0223/$18.50/0

Printed in the United States of America

SRS RADIATION INDUCED POLYMERIZATION OF 2,4-HEXADIYNEDIOL-BIS-(p-TOLUENESULPHONATE) (PTS)

MICHAEL DUDLEY AND JOHN N SHERWOOD
Department of Pure and Applied Chemistry, University of Strathclyde, 295 Cathedral Street, GLASGOW G1 1XL Scotland

and

DAVID J ANDO AND DAVID BLOOR
Department of Physics, Queen Mary College, University of London, Mile End Road, LONDON E1 4NS, England

Abstract An assessment has been made of the defect structure of single crystalline 2,4 Hexadiyne diol-bis-(p-toluene sulphonate) (PTS) both in the monomer and polymer form, using White Beam Synchrotron Radiation Topography. A one to one relationship was found between defects present in the monomer and subsequent polymer crystal. The strain induced during the polymerization process has also been recorded. This strain which builds up during the initial stages of polymerization, relaxes when polymerization is complete, to leave a polymer crystal with the defect structure of the original monomer crystal 'frozen in'. No evidence was found for an influence of growth dislocations on the radiation induced polymerization process.

INTRODUCTION

Currently there is widespread interest in the process of solid state polymerization in diacetylene single crystals. Some of this interest has been directed towards the definition of the dislocation structure in these materials in order to ascertain the role of defects in this process.

Using etching techniques, Schermann, Wegner, Williams and Thomas[1] located the emergent ends of dislocations on (100) and (102) surfaces of PTS monomer crystals and demon-

strated their potential role as nucleation centres for thermally induced polymerization. Partial confirmation of their assignment of Burgers vector and line direction to the dislocations has come from the transmission electron microscopic studies of Young and Peterman[2], who identified edge dislocations of Burgers vector [010] emergent on the (100) faces of thin specimens.

An alternative technique for this purpose is X-ray Topography[3]. This has the additional advantage that it can be used to differentiate between bulk and surface defects in large specimens of high quality. Hence it allows a judgement to be made of the role of both types of defect structure in any subsequent processes.

To date, studies using conventional X-ray topographic techniques have revealed gross defect structures with no resolution of individual defects[4,5]. Progress in this field has been aided by the advent of the highly versatile White Beam Synchrotron Radiation Topography technique[6], which is tolerant of a greater degree of lattice distortion, and by the successful growth of large monomer single crystals of a quality which surpasses that of previously available samples[7].

In a recent paper[8] we have confirmed the high degree of crystallinity of PTS polymer using White Beam Radiation Topography (WBRT) and a Synchrotron source. This, coupled with the insensitivity of the material to radiation damage and the shorter exposures in the high intensity beam makes the method ideal for the examination of the defect structure of monomer and polymer crystals and of the possible changes in defect structure during the course of the polymerization process. We have pursued these experiments and report, for the first time, details of the relationship be-

tween the dislocation structure of monomer and polymer crystals of PTS. This paper amplifies results presented in a previous short report[9].

The WBRT technique makes use of the high intensity, broad spectrum radiation, emitted from a synchrotron source. In the experiment, the crystal is orientated in the incident beam and the detector (film, photographic plate or TV imaging system) placed on a pre-set position to record the diffracted beam. The experiment can be carried out in transmission or back reflection as shown in Figure 1. These diffracted beams arise from sets of planes (hkl) with interplanar spacings d which satisfy the Bragg equation

$$(n)\lambda = 2d \sin\Theta$$

for particular wavelength λ in the spectral range of the incident beam. Θ is the angle of incidence.

The diameter of the incident beam ($\sim$2.5cm) is large

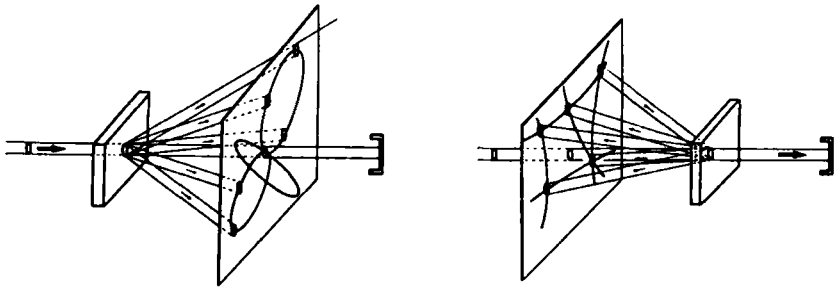

a b

FIGURE 1. Experimental Geometry for White Beam Synchrotron Radiation Topography - Laue Geometry a) transmission b) reflection

compared with the dimensions of most crystals and the beam divergence is low. Thus, each diffracted spot is potentially an X-ray topograph of the whole crystal.

As in conventional topography any defect which causes a departure from perfection in the crystalline lattice may show up as a contrast variation in the image on the detector. The technique is capable of imaging dislocations, precipitates, grain boundaries, twins stacking faults, magnetic and ferroelectric domains, growth sector boundaries etc. The overall resolution, which depends on the geometry of the source is $\sim$2μm at the Synchrotron Radiation Source (SRS) at Daresbury, UK. The typical dislocation image width is $\sim$5-15μm (cf $\sim$5-10nm for electron microscopy). This sets an upper limit to the dislocation densities which can be usefully studied at $<10^6 cm^{-2}$. A figure of $<10^2 cm^{-2}$ is more desirable. Although only potentially equivalent in resolution to that attainable using monochromatic laboratory sources, the broad spectral range of the radiation places less constraint on specimen quality. Whereas specimens of extremely high quality (mosaic spread <90" arc) are required for the former technique, much greater deviations can be successfully recorded as a single image by the white beam technique. In fact, specimens with gross disorder, polycrystals, twinning etc. can be successfully and usefully recorded in full but divided images.

The experiment may be carried out in two geometries.

a) With the crystal orientated in the beam to select a particular incident wavelength and the detector placed in transmission with the corresponding 2θ angle so that its area is normal to the diffracted beam. In this way, the detailed defect structure of a particular diffraction image may be recorded and followed. This arrangement provides

the minimum geometrical distortion of the image.

b) With one set of crystal planes and the detector area normal to the incident beam (Figure 1). Now, with a large area photographic plate, a number of images can be recorded simultaneously (Figures 1 and 3) and variations in crystal structure can be examined in parallel with sub-structural changes. Due to the high angle of projection the images are more distorted than in the Bragg case.

In the present studies, the latter method of recording was used as it allowed the rapid monitoring of gross structural changes as the crystal converted from monomer to polymer. At the same time, from each successive photograph the internal dislocation structure could be defined.

EXPERIMENTAL

MATERIALS

PTS monomer was purified by successive crystallizations from pure acetone. Single crystals (1x1x0.5cm^3) were grown by slow, controlled evaporation of saturated acetone solutions of the monomer at 298 ± 1K.

The resulting monomer crystals were pale-red in colour and exhibited the morphology (100), (001), (111), $(1\bar{1}1)$, $(1\bar{1}\bar{1})$, $(11\bar{1})$ shown schematically in Figure 2. They were transparent and free from visible imperfections.

Both PTS monomer and polymer crystallize in the monoclinic space group $P2_{1/c}$[10] with:

monomer: a = 1.460nm, b = 0.515nm, c = 1.502nm and β = 118.4°

polymer: a = 1.449nm, b = 0.491nm, c = 1.494nm and β = 118.14°

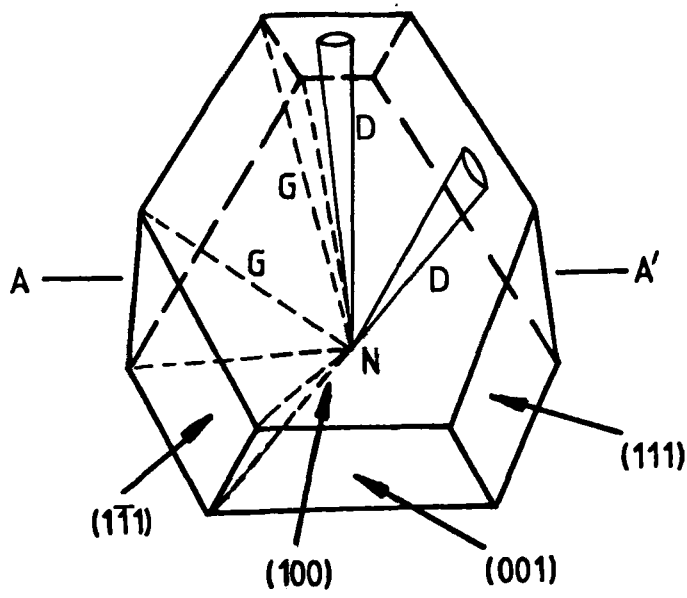

FIGURE 2. Schematic diagram of the morphology of PTS showing growth sector boundaries G, and dislocation bundles D emanating towards selected facets from the nucleation point N

TOPOGRAPHIC EXPERIMENTS

In these experiments the radiation from the SRS was used for two purposes

a) As the investigative probe

b) As the driving force for polymerization

Topographs were taken in the Laue configuration of crystals cleaved parallel to the (100) face with the radiation incident normal to this face. For detailed sub-structural examination image patterns were recorded as Agfa Structurix D2 film with exposures of the order of 2-3 minutes (Beam

current ∿260ma, 2GeV). More rapid (∿ 10s) exposures on Polaroid film were taken to monitor the kinetic progress of the polymerization process. In both cases, Laue patterns were recorded sequentially following successive irradiation periods.

The absorbed radiation dose was ∿7Mrad s^{-1} and the wavelength spread of the incident radiation 0.03-0.3nm.

RESULTS

Initial experiments at room temperature (successive 3 min exposures) showed that the polymerization process initiated during the first exposure and progressed to completion in 6 minutes. During this exposure the initially pale-red crystal, darkened and developed the characteristic metallic gold colour expected for this polymer.

Simultaneously, the 1cm diameter crystal deformed to become concave to the incident beam and reached a maximum curvature of ∿1cm radius after 3 minutes. On continued irradiation the crystal relaxed back to planarity in the succeeding 3 minutes. We believe that this massive deformation arises from strains set up in the surface regions of the monomer crystal in the initial stages of the reaction. The distribution of absorbed radiation is such that the radiation dose in the near surface regions is massive (2.6Mrad s^{-1} in the first 0.01cm). Hence reaction will initiate here. The curvature, principally around the c direction, is consistent with the relative changes in lattice parameter on polymerization.

On continued irradiation, the accumulated dose (and hence polymerization) in the bulk evens out the strain and the crystal straightens. Rather surprisingly, this massive

deformation produces no apparent deterioration in the quality of the crystal. The final polymer crystal is strain free.

The development of gross structural and sub-structural effects during the polymerization process was followed dynamically by short successive exposures on Polaroid film. Selected examples from a full sequence of 30, ∿6 second exposures are shown in Figure 3.

The first picture at 7Mrad cumulative dose shows the diffraction pattern of the monomer. The images are clean and well-defined and confirm the high structural perfection of the monomer crystals before polymerization. As irradiation continues, the onset of polymerization is accompanied by a development of considerable asterism in the images which results in their 'streaking' across the plate. As the polymerization approaches completion, the asterism diminishes until at complete conversion (∿716Mrad) a well-defined pattern corresponding to the polymer structure is obtained. We note at this stage that polymerization only occurs during irradiation and any post-irradiation polymerization is too slow to be discernible.

The asterism noted can be associated with the development of internal strain alone. The influence of crystal curvature and general radiation damage can be ruled out. In cases where radiation induced curvature can be provoked

FIGURE 3. Selected examples from a series of normal Laue patterns of PTS taken on Polaroid film, recording the polymerization process after cumulative irradiation doses of (a) 77Mrad (b) 185Mrad (c) 259Mrad (d) 458Mrad (e) 551 Mrad (f) 619Mrad (g) 653Mrad (h) 716Mrad

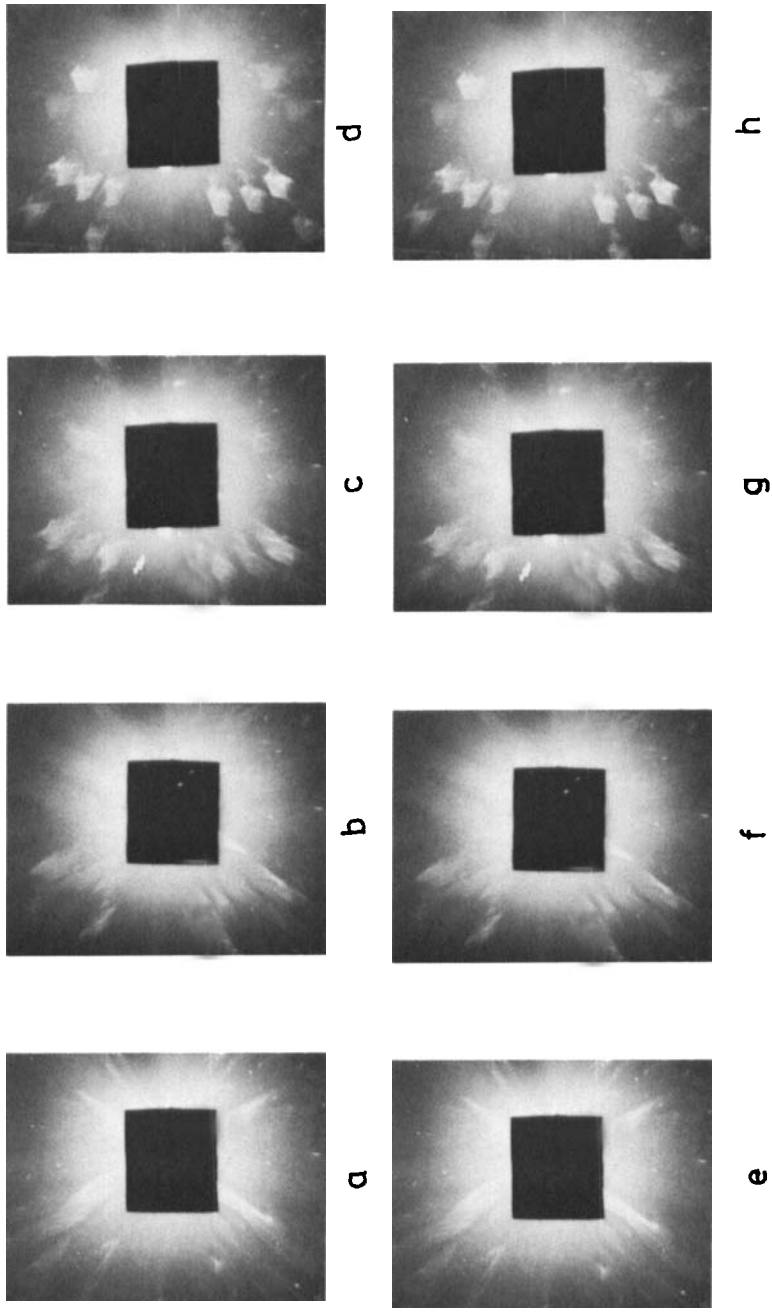

Figure 3

but where the subsequent reaction does not yield a second solid phase e.g. ammonium perchlorate[11], the image size changes but not its position on the Laue pattern. General radiation damage inevitably yields scattering centres which give a considerably darkened image[11]. Neither change was observed in the present case.

The regular distribution of asterism implies an 'isotropic' distribution of strain in the sample rather than it being dominantly aligned. We estimate this strain to correspond to $\Delta d/d = 3 \times 10^{-2}$, where d is an average lattice spacing.

Whereas the Polaroid film is satisfactory for following gross structural changes, the resolution is insufficient for detailed analysis. This can be achieved using the finer grain D2 film.

Figures 4a and b compare equivalent $0\bar{1}1$ reflections from Laue topographs of a (100) cleaved slice of high quality PTS crystal both before and after polymerization. Figure 4c, a $1\bar{1}\bar{2}$ reflection, shows the better definition which can be achieved under more ideal diffraction conditions (higher structure factor, different wavelength, absorption).

All examples show the characteristic defect structure associated with crystals grown from saturated solution by self-nucleation. From the nucleation centre N, dislocations of a variety of characters propagate towards the central area of each face (e.g. D, Figure 2). Dislocations may also form at inclusions I incorporated during growth. These will also propagate towards the bounding facet of the growth sector in which they form. Additionally, the slight lattice mismatch which distinguishes one growth sector from another results in strain which also becomes imaged as a growth sector boundary G (dotted on Figure 2). Cleavage of a (100)

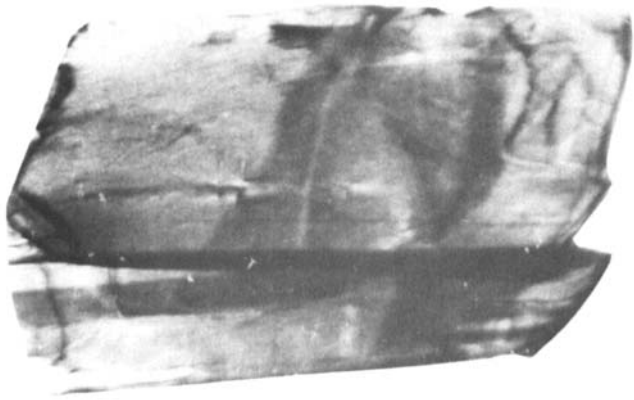

a

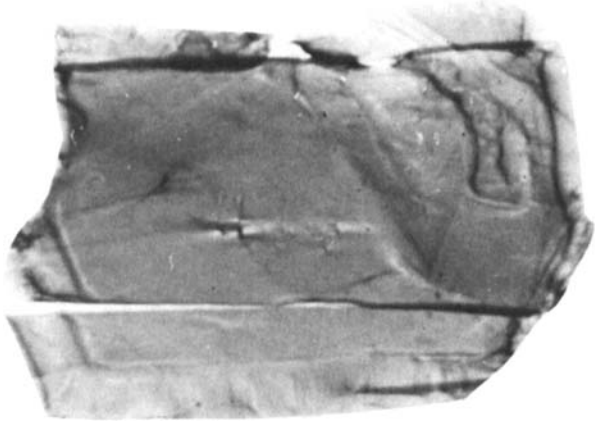

b

FIGURE 4.

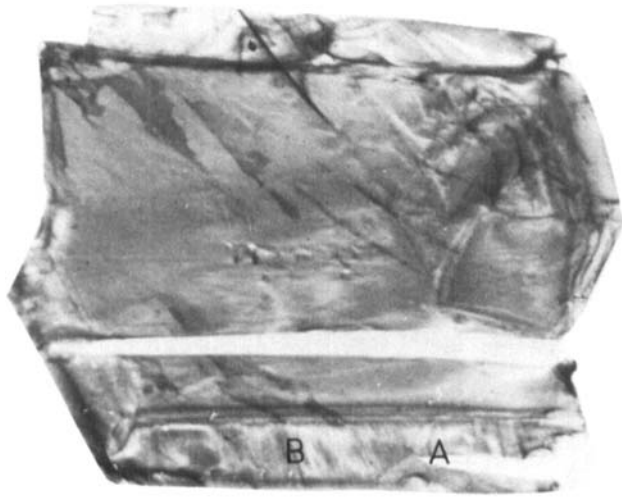

c

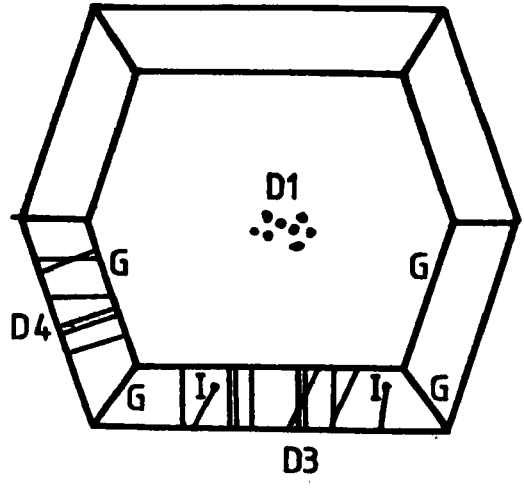

d

FIGURE 4 (contd.)

FIGURE 4. White Beam Synchrotron topographs of PTS
(a) $0\bar{1}1$ reflection from the monomer $\lambda = 1.25\mathring{A}$
(b) $0\bar{1}1$ reflection from the polymer $\lambda = 1.12\mathring{A}$
(c) $1\bar{1}\bar{2}$ reflection from the polymer $\lambda = 1\mathring{A}$
(d) Schematic representation of the distribution of dislocations D and growth sector boundaries G in a (100) cleaved section of PTS.
The different operative wavelengths in (a) and (b) arise from the slightly different diffraction geometries adopted before and after polymerization. The image shapes are distorted due to the non-normal incidence of the particular diffracted beam on the detector, characteristic of a normal Laue pattern type geometry (scale mark 5mm)

section (e.g. AA', Figure 2) will thus yield the distribution of defects shown in Figure 4d.

Comparison of the topographs with Figure 4d shows that this general distribution does occur. Bundles of dislocations D emerge normal to the (100) surface. These are evident on the topographs by the lobed dynamical contrast associated with the surface relaxation of the emerging dislocations. No other dislocations can be seen in the (100) growth sector.

In contrast, the faster grown {111} growth sectors contain many more dislocations. Their distribution across the width of the sector suggests that many have formed at inclusions incorporated during growth. This implies a ready deformation. There is a wide distribution of line directions both normal (A) to and at acute angles (B) to the bounding facet. This implies that these comprise both pure edge and screw (A) and mixed (B) dislocations. A com-

plete analysis of the nature and character of these dislocations is in progress.

Of over-riding interest at present is the close similarity between the dislocation structure of the monomer and polymer crystals. Thus, in spite of the considerable strain which develops during the polymerization process, there is little or no multiplication of growth dislocations or generation of mechanically introduced dislocations. The polymerization process effectively 'freezes in' the defect structure of the monomer.

This distribution of defects could be useful since we can identify growth sectors of high and low (∿zero) dislocation content. If growth dislocations do, as proposed, influence the polymerization process, then we would expect to see an enhanced reactivity in the more defective regions. Up to the present time we have found no evidence for such a distinction. Within the time scale of the experiment all growth sectors react at equivalent rates.

The work is proceeding to define the nature of the dislocation structure and other defects in these and other diacetylene crystals and the role of defects in the polymerization process.

SUMMARY

Using white beam synchrotron radiation topography an assessment has been made of the degree of strain which develops in PTS monomer crystals during X-radiation induced polymerization. The defect structure of the monomer crystals has been imaged and has been shown to be retained in the polymer crystal. No evidence was found for an influence of dislocations on the polymerization process.

ACKNOWLEDGEMENTS

We thank the SERC for the financial support of this programme. The help of the Staff of the SERC Daresbury Laboratory in the performance of the experiments is gratefully acknowledged.

REFERENCES

1. W. Schermann, G. Wegner, J.O. Williams and J.M. Thomas, J. Polymer Sci., Polymer Phys., Ed. 13 753 (1975).
2. R.J. Young and J. Petermann, Makromol. Chem., 182 621 (1981).
3. Characterization of Crystal Growth Defects by X-ray Methods, Eds. B.K. Tanner and D.K. Bowen, Nato A.S.I. series B, Physics Vol. 63, Plenum NY (1980).
4. J.M. Schultz, J. Mat Sci., 12 2258 (1977).
5. R.G. Rosenmeier, R.E. Green Jr. and R.H. Baughman, J. Appl. Phys. 52 7129 (1981).
6. J. Miltat in Reference 3, p401.
7. M. Dudley and J.N. Sherwood, to be published.
8. D. Bloor, D.K. Bowen, S.T. Davies, K.J. Roberts and J.N. Sherwood, J. Mat. Sci. Lett. 1 150 (1982).
9. M. Dudley, J.N. Sherwood, D.J. Ando and D. Bloor, J. Mat. Sci. Lett. 1 479 (1982).
10. Von D. Kobelt and E.F. Paulus, Acta Cryst. B30 232 (1974).
11. H.L. Bhat, D.B. Sheen, J.N. Sherwood and P.J. Herley, to be published 1983.